Proceedings of the 2015 ASME Turbo Expo
Turbo Expo 2015
June 15-19, 2015, Montreal, Quebec, Canada

GT2015-42055

FIBER LASER DEPOSITION OF NICKEL-BASED SUPERALLOYS USING FILLER WIRE FEED

Y.N. Zhang
National Research Council of Canada
Montréal, QC, Canada

***X. Cao**
National Research Council of Canada
Montréal, QC, Canada
(*Corresponding author: xinjin.cao@cnrc-nrc.gc.ca)

P. Wanjara
National Research Council of Canada
Montréal, QC, Canada

ABSTRACT

In this work, a continuous wave fiber laser welding system was used to deposit nickel-based superalloys Inconel 718 (IN 718) and Waspaloy using filler wire feed sources. The multi-bead and multi-layer deposits that were manufactured were characterized in terms of the macro- and microstructures, defects, and hardness in both the as-deposited and fully heat treated conditions. The tensile properties of the deposits in the heat treated condition were also determined and compared to the existing aerospace materials specifications. Using optimized laser processing parameters, high strength deposits could be manufactured, though minor weld metal liquation cracking for IN718 and strain-age cracking for Waspaloy were present, which compromised slightly the ductility as compared to wrought aerospace specifications for the two alloys. The successful development of the direct laser deposition process using wire feeding indicates the potential of employing the fiber laser technology to manufacture nickel-based superalloy aerospace components.

INTRODUCTION

Direct laser deposition is an emerging technology for manufacturing near-net shaped aerospace parts from value added materials, such as nickel-based superalloys, for aero-engine sub-assemblies or components [1-3]. During direct laser deposition, the filler material is fed in the form of either powder or wire, but the latter is lower in cost with greater material efficiency (reduced waste), lower contamination levels (higher quality), lower oxidized contaminants (fewer defects) and superior deposition rates (productivity) [4-7]. Despite the current good understanding of the phase constituents and mechanical performance of the laser deposited superalloys (IN718 and Waspaloy), information on high power continuous wave fiber laser manufacturing using wire feeding is still limited. Compared to the conventional CO_2 and Nd:YAG lasers, the current generation of high power fiber lasers are reliable, low-cost and efficient with a good beam quality, power scalability, flexible fiber beam delivery, small footprint, good process versatility and automation capacity [8-11]. Hence in this study, direct laser deposition was performed using IN718 and Waspaloy filler wires with the objective to substantiate the process feasibility using a high power continuous wave (CW) fiber laser for applications in aerospace. The macrostructure, defects, microstructure and mechanical properties of the IN718 and Waspaloy deposits were characterized in both the as-deposited and the post-deposition heat treated (PDHT) conditions.

EXPERIMENTAL PROCEDURES

In the present research, laser deposition was conducted using an IPG Photonics 5 kW CW solid-state Yb-fiber laser system (YLR-5000) mounted on an ABB robot. A collimation lens of 150 mm, a focal lens of 250 mm and a fiber diameter of 600 µm were employed to produce a nominal focusing spot diameter of roughly 1.0 mm. A positive defocusing distance of +12 mm was used to obtain a laser power density of about 792 W/mm^2. The main laser processing parameters were set at a laser power of 1.4 kW, advancing speed of 0.3 m/min and wire feed rate of 0.6 m/min. The bead spacing was 1.5 mm and the interlayer distance was 0.7 mm. The laser head was inclined 2-

3°, both along the lateral side and from the vertical position towards the scanning direction, to avoid any damage to the equipment from a laser beam reflection. The fiber laser beam, with a wavelength of about 1.07 µm, was positioned on the top surface of the deposit. To better protect the molten metal and solidified material from oxidation during laser deposition, the deposited material was shielded using two flow streams of Ar gas. One stream of Ar gas, at a flow rate of 30 cfh (2.36 x 10^{-4} m^3/s), was directed towards the scanning direction at an angle of 18-20° to the deposit surface, while the other was directed opposite to the scanning direction at a flow rate of 20 cfh (1.57 x 10^{-4} m^3/s). The IN718 and Waspaloy filler wires, supplied by Haynes International Inc., were ~0.89 mm in diameter and had a nominal composition as given in Table 1. Both the IN718 and Waspaloy filler wires were axially fed from the laser scanning direction at an inclination angle of 30° from the top surface of the deposit where interception with the incident laser beam occurred. Fig. 1 schematically shows the experimental setup of the laser deposition system used in this study [12]. The as-received substrate material was extracted directly from a service-exposed and failed IN718 aerospace component, which was assumed to be solution heat treated and aged before used.

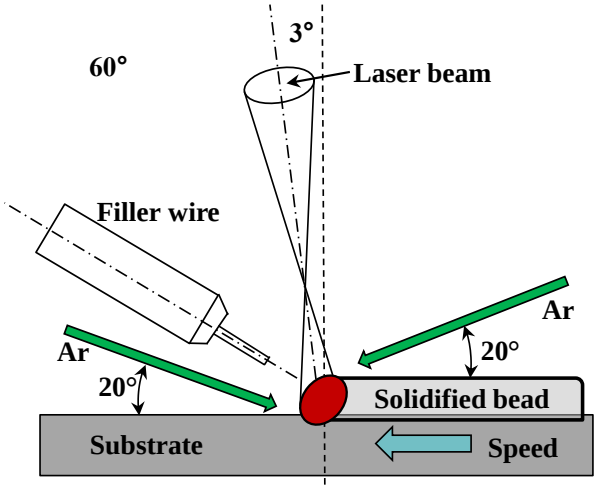

Fig. 1. Schematic diagram showing the laser deposition system used in this study [12]

After laser deposition, the IN718 and Waspaloy deposits were solution heat treated and aged (STA). For the IN718 deposits, the solution heat treatment was performed in vacuum at a temperature of 954°C (1750 ± 25°F) for 1 h in the presence of inert Ar gas and then cooled (with Ar) at a minimum rate of 16.7°C/min^{-1} (30°F·min^{-1}) to a temperature of 538°C (1000°F) followed by rapid cooling in Ar. The aging consisted of the following steps: heating to 732°C (1350 ± 25°F), soaking for 8 hours, furnace cooling under Ar to 599°C (1110 ± 25°F) and holding for 8 hours, and finally Ar quenching. The solution heat treatment for the Waspaloy deposit was carried out in vacuum at a temperature of 1005°C to 1020°C (1841°F to 1868°F) for 1 hour, followed by cooling with inert gas Ar to a temperature of 599°C (1110°F) within 18 minutes, and then cooling to a temperature of 299°C (570°F) in Ar. The aging consisted of the following steps: heating to 840°C to 860°C (1544°F to 1580°F), soaking for 4 hours in vacuum, furnace cooling under Ar to 750°C to 770°C (1382°F to 1418°F), holding for 16 hours in vacuum, and finally Ar quenching.

Metallographic samples of the IN718 and Waspaloy deposits were extracted in both the as-deposited and PDHT conditions. Specifically, both the IN718 and Waspaloy deposits were sectioned transverse to the scanning direction using a precision cut-off saw to extract specimens for metallographic preparation. After sectioning, the specimens were mounted, ground and polished to a surface finish of 0.04 µm, followed by electrolytic etching in a saturated solution of 10 g oxalic acid in 100 ml distilled water using a voltage of 6 V for 8-20 seconds, depending on the alloy chemistry and heat treatment conditions. Optical microscopy (OM) on an Olympus GX-71 system was used to examine the macro- and microstructural features in the deposited zone.

The hardness was measured using a load of 300 g and a dwell period of 15 seconds on a Vickers microhardness (HV) machine (Struers Duramin A300), equipped with a fully automated testing cycle (stage, load, focus, measure). At an indent interval of 0.2 mm, at least three hardness lines were measured to determine the average hardness of each deposit. Also, bulk hardness measurements were conducted using a Wilson Rockwell tester to evaluate the Rockwell hardness of the deposits. Standard tensile samples with a gauge length of 16.26 mm (0.640" ± 0.005") and a diameter of 4.06 mm (0.160" ± 0.003") were machined in accordance with ASTM-E8-04 from the IN718 and Waspaloy deposits. Using a United SFM-30 system, room temperature tensile testing was conducted at a strain rate of 8.3×10^{-5} s^{-1} before the yield point and 8.3×10^{-4} s^{-1} after yielding.

Table 1 Nominal and measured compositions of IN718 and Waspaloy laser deposits (wt. %)

Elements	Ni	Cr	Fe	Co	Nb	Mo	Ti	Al	C	Mn	Si	B	Cu
[1]IN718 filler wire	52	18	19	1	5	3	0.9	0.5	0.05	0.35	0.35	0.009	0.1
[2]DLD IN718	50.2	18.6	19.4	1	4.9	2.9	1.3	-	-	-	0.22	-	-
[1]Waspaloy filler wire	54.0	19.5	2.0	13.5	-	4.3	3.0	1.3	0.08	0.10	0.15	0.01	0.1

Note: [1]Individual values represent the upper limit for the nominal composition; [2]Measured values using an Olympus Delta X-Ray Fluorescence (XRF) analyzer at a beam voltage of 40 V and current of 35A

RESULTS AND DISCUSSION

MACRO- AND MICROSTRUCTURES

As shown in Fig. 2, the multi-bead and multi-layer deposits of IN718 and Waspaloy contain no visible macroporosity and/or macrocracks under optimized process conditions using a high power fiber laser and wire feed addition. In both deposits, typical equiaxed or elongated dendritic structures were observed, as shown in Figs. 3 and 4. IN718 and Waspaloy, being heavily alloyed materials, solidify in a dendritic mode after direct laser deposition. The dendrites extend from the bead interface to the bead center. In laser deposition, the relatively rapid cooling rate leads to fine structures in the deposits and extended solute solubility [1], which can reduce the extent of segregation and cause the formation of less eutectic constituents. During solidification of IN718, the elements Nb, Ti and Mo accumulate at the front of the liquid/solid interface and segregate into interdendritic areas where carbide (NbC, fcc) and Laves particles may form [1], as shown in Figs. 3a and 4a. In addition, the γ and NbC eutectic is suppressed during rapid cooling [13]. In the PDHT condition dissolution of the Laves particles occurs at a solution temperature of 954°C. In this case, less interdendritic constituents were observed, as shown in Figs. 3c and 4c. Furthermore, the needle-like Ni_3Nb-δ phase may precipitate around the Laves particles in the interdendritic regions due to the partial dissolution of the Laves particles during the heating stage of the solution heat treatment. However, the solution treatment conducted at 954°C did not completely dissolve the Laves phases. Therefore, during the solution heating treatment, some local regions around the Laves particles in the deposited metal may have a sufficient Nb concentration to incite the formation of the needle-like δ and γ″ phases.

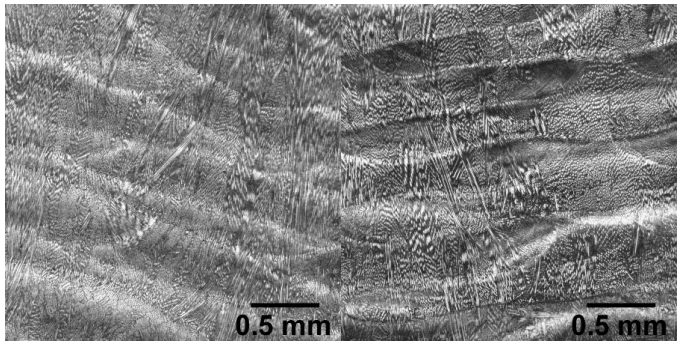

(a) IN718 deposit (b) Waspaloy deposit

Fig. 2 Macrostructures of the multi-layer deposits in as-deposited condition

In the Waspaloy deposit (Fig. 3b), γ′ and MC carbides in interdendritic regions are selectively etched (darkened), as compared to the dendritic cores. Though the γ′ precipitate phase was too small to be discerned using optical microscope, typically about 30 vol. % γ′ can be found in conventionally cast Waspaloy [1]. It was reported that this amount can be reduced to less than 20 vol. % at rapid solidification rate, as experienced during laser welding. Therefore, the Waspaloy deposit, most likely, contains less than 30 vol. % γ′ [1]. Furthermore, the dendrites were observed to be finer and more equiaxed in each bead center (Fig. 3) but became slightly coarser and more columnar near the bead interface (Fig. 4). Fine equiaxed dendritic growth in the bead interior gives rise to more, but smaller and well-separated, interdendritic regions, which lead to the formation of relatively fine and discrete secondary particles. In contrast, columnar dendritic growth adjacent to the bead interface results in fewer, but larger and more continuous, interdendritic regions, and thereby coarser and more interconnected secondary particles [13, 14].

As is well known, the cooling rate over the solidification temperature range can be estimated using the following equation [15, 16]:

$$\lambda s = k_s \Theta^n \quad \text{.....(1)}$$

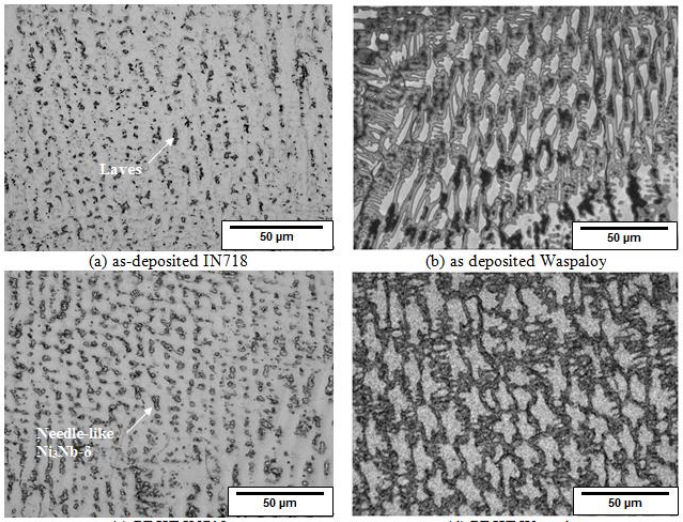

Fig. 3 Microstructures of the deposits at a bead center

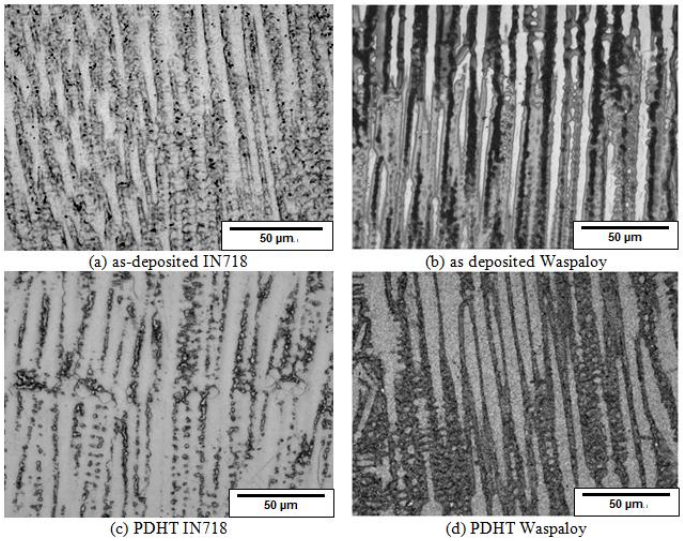

Fig. 4 Microstructures of the deposits near a bead interface

Where Θ is the cooling rate over the solidification temperature range, and k_s and n are constants. The deposits in Fig. 4 consists of a dendritic microstructure with an average secondary dendrite arm spacing, λs, of ~ 3.3 ± 0.5 μm for IN718 and 3.0 ± 0.4 μm for Waspaloy, as measured near the bead interfaces. Using the values of $k_s = 4.7 \times 10^{-2}$ mm·$K^{1/3}s^{-1/3}$ and n = -0.4, as experimentally determined for a nickel-based superalloy (IN738) [13], the cooling rates near the bead interface were estimated to be ~971 K/s for IN718 and ~1267 K/s for Waspaloy. The different cooling rates obtained for IN718 and Waspaloy may be related to the difference in their physical properties. Regardless, these cooling rates are quite similar to that obtained for CO_2 laser welded Haynes® 282 alloy, where the secondary dendrite arm spacing and the cooling rate within the fusion zone were 3.1 ± 0.6 μm and 1168 K/s, respectively [15]. It is noteworthy that these cooling rates are representative of the local values over the solidification temperature range near the bead interface. In contrast, the bead center has a lower cooling rate as compared with the bead interface [17]. Nonetheless, the cooling rates calculated in the present study are twice that reported for gas tungsten arc welded IN718 (500 K/s) [18].

DEPOSITION DEFFECTS

Weld metal liquation cracking in IN718 deposits:

Some interlayer microcracks were frequently present in the lower beads near the layer interface in the as-deposited condition, as shown in Fig. 5. These regions in the lower beads act as the heat-affected zone (HAZ) of the adjacent upper layer beads that are deposited subsequently. Therefore, these microcracks are quite similar to the HAZ microfissures or liquation cracks that are widely encountered in IN718 welds and are usually termed as weld metal liquation cracking in multi-pass welding [1, 10]. As shown in Fig. 5a and 5b, weld metal liquation cracking occurs in the lower beads near the interfacial area, but the cracks can propagate along the bead interface and even extend into the upper newly deposited beads. The presence of the liquation cracks can be reasoned on the basis of the cast structure in the deposits and the formation of both the Nb-rich carbides and Laves phase during the final stages of solidification. For cast IN718, it is known that liquation cracking is dominated by the melting of the Laves phase rather than constitutional liquation of the Nb-rich carbides, since the former precipitates at a lower temperature and the latter is much lower in amount [1, 13, 14]. Hence, when a previously deposited bead is reheated during deposition of a subsequent pass, the solidification grain boundaries in the lower beads adjacent to the layer interface may remelt and thus form liquated boundaries. The reheating may also promote grain growth, resulting in the formation of migrated grain boundaries along which liquation and even cracking may occur [1, 19]. In the PDHT condition, weld metal liquation cracking appears to partially recover, as shown in Fig. 5c and 5d, probably due to several reasons: (i) the dissolution of the Laves phases during the solution heat treatment at the heating stage leads to the release of Nb into the matrix and the formation of the γ" strengthening phases, (ii) the lack of the Laves phase and NbC phases at the grain boundaries, which discourages the constitutional liquation and penetration mechanism, and (iii) the thermal strains and high shrinkage stresses caused by rapid solidification that can be released during the PDHT [1, 11].

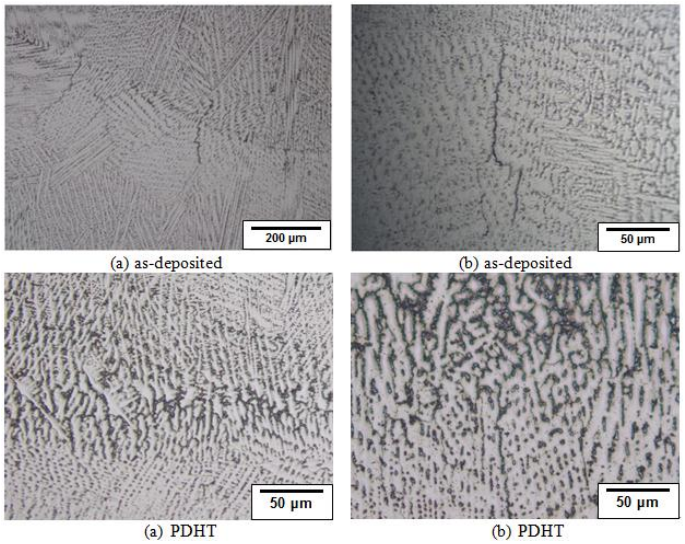

Fig. 5 Weld metal liquation cracking in a multi-bead and multi-layer deposit of IN718

Strain-age cracking in Waspaloy deposits:

The main defect observed in the Wapaloy deposits was microcracks. As shown in Fig. 6, the microcracks originated in the reheated zone of the previously deposited beads (similar to the HAZ of the subsequently deposited beads) and then extended to the subsequently deposited material in both the as-deposited and PDHT conditions. Typically, nickel-based superalloys are predominantly susceptible to two forms of solid-state cracking, namely ductility-dip cracking and strain-age cracking (SAC). In SAC, a solid-state crack usually appears at a temperature between the solidus and roughly half of the melting temperature of the material, which is typically encountered during reheating in multi-pass welds or during post-weld heat treatment (PWHT) [1, 20]. Considering the nature of the laser deposition process, the cracks observed in the Waspaloy deposits are reasonably assumed to be SAC due to repeated reheating during multi-pass processing and/or post-deposition heat treatment [1, 20]. It is noteworthy that SAC resistance in nickel-based superalloys is generally attributed to the rate and nature of the precipitation reaction that promotes strengthening, particularly for γ′-Ni_3(Al,Ti) strengthened alloys. In this regard, IN718 has a greater resistance to SAC than Waspaloy due to the slower aging rate and the beneficial effects of γ″ versus γ′ precipitation during PWHT [1]. Notwithstanding the inherent limitations in the weldability of both these superalloys, the successful deposition of integral IN718 and Waspaloy deposits with no visible macropores but only some minor weld metal liquation cracking (IN718) or strain-age cracking (Waspaloy) indicates the good potential of using wire

feeding with the fiber laser deposition technology to manufacture superalloy components for aerospace applications.

Microindentation hardness

As indicated in Table 2, the average hardness of the IN718 and Waspaloy deposits was 291 HV (IN718) and 322 HV (Waspaloy) in the as-deposited and 490 HV (IN718) and 400 HV (Waspaloy) in the PDHT conditions. The difference in the hardness for each alloy in the as-deposited and PDHT conditions is mainly related to the amount of coherent γ' and γ" phase for IN718 and γ' phase for Waspaloy, respectively. The precipitation of the strengthening phase γ" and/or γ′ is hindered during laser deposition due to the relatively rapid thermal cycle, which thus necessitates the post-deposition aging treatment. The Rockwell hardness of the deposits was 23.6 HRC (IN718) and 26.8 HRC (Waspaloy) in the as-deposited condition and 41.6 HRC (IN718) and 35 HRC (Waspaloy) in the PDHT condition (Table 2). The hardness of both alloys in the PDHT condition was greater than the minimum requirements in the AMS 5596K and AMS 5544J specifications.

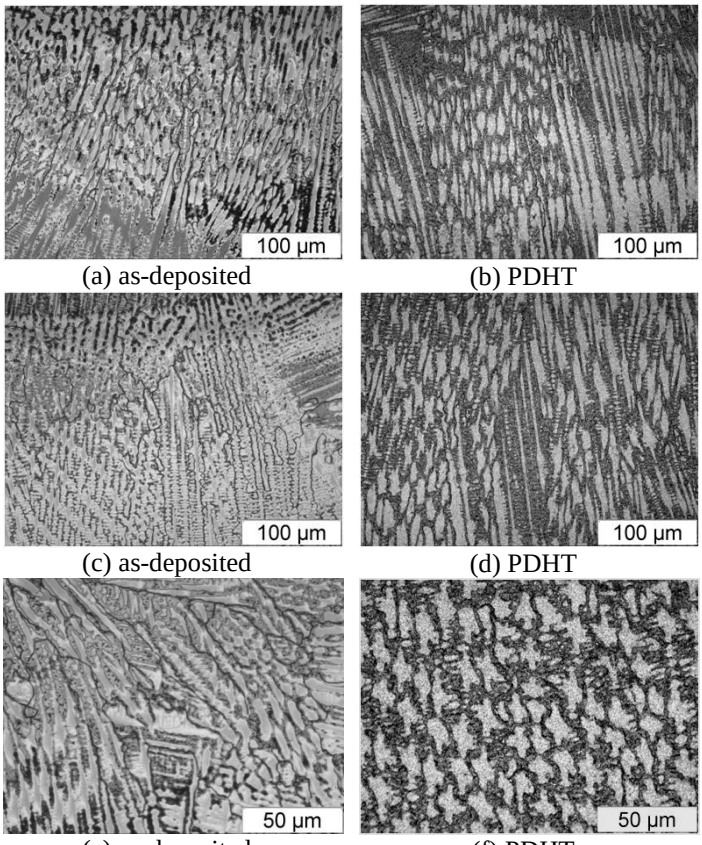

(a) as-deposited (b) PDHT
(c) as-deposited (d) PDHT
(e) as-deposited (f) PDHT

Fig. 6 Strain-age cracks in the reheated zones of the previous beads and the deposits of the subsequent beads of the Waspaloy deposits

Table 2 Hardness of IN718 and Waspaloy deposits

Conditions	HV 300 gf, 15 s	HRC	AMS 5596K*/5544J** HRC (min)
IN718 in as-deposited condition	291 ± 18	23.6	-
Waspaloy in as-deposited condition	322 ± 12	26.8	-
IN718 in PDHT condition	490 ± 18	41.6	*36
Waspaloy in PDHT condition	400 ± 11	35.0	**34

Tensile properties

As shown in Table 3, the overall room temperature tensile strength properties, i.e. the yield strength (YS) and ultimate tensile strength (UTS), of the laser deposited IN718 and Waspaloy were well above the minimum requirements as defined in the AMS 5596K and AMS 5544J specifications, respectively. However, the ductility values of the IN718 and Waspaloy deposits were slightly lower than the respective minimum requirements as defined in these specifications. Therefore, the lower ductility is the primary concern for the additive manufacturing of IN718 and Waspaloy. One of the main reasons for the low ductility may be attributed to the metallurgical defects, e.g. weld metal liquation cracking for IN718 and strain-age cracking for Waspaloy. Notwithstanding the slightly lower ductility, it is noteworthy that both the AMS 5596K and AMS 5544J specifications are for wrought alloys. A more realistic target for the ductility of laser deposited nickel-based superalloys could then probably be drawn from specifications for cast grades. For instance, IN738 has typical elongation and reduction in area of 7% and 9%, respectively [21]. Characterization of the other mechanical properties of the laser deposited samples, including elevated temperature tensile strength and ductility, creep, rupture strength and life, and fatigue properties is the topic of a current research study that will be relayed in the near future.

Table 3 Room temperature tensile properties of IN718 and Waspaloy in PDHT condition

Tensile properties	IN718 DLD	AMS 5596K (IN718)	Waspaloy DLD	AMS 5544J (Waspaloy)
UTS (MPa)	1321.0	≥ 1241.1	1260.4	≥ 1207
YS (MPa)	1097.6	≥ 1034.2	815.0	≥ 793
El. in 4D (%)	9.8	≥ 12	19.0	≥ 20
RA (%)	11.5		24.5	

CONCLUSIONS

- As a variant of multi-pass welding process, direct laser deposition has similar metallurgical defects, e.g. weld metal liquation cracking for Inconel 718 and strain-age cracking for Waspaloy.
- Weld metal liquation cracking is frequently observed in the lower (previous) beads near the interlayer interface in the as-deposited condition using Inconel 718 filler wire. The cracks can propagate along the grain boundaries and even extend across the interface into the subsequently deposited upper beads.
- The marginally high (Ti + Al) content for Waspaloy results in a high volume faction of γ' that provides high strength at elevated temperatures but also exacerbates the strain-age cracking during reheating stage of the direct laser deposition process and/or the post-deposition heat treatment.
- The hardness of the Inconel 718 and Waspaloy laser deposits was lower in the as-deposited condition. A post-deposition solution heat treatment and aging cycle was observed to recover the hardness to a value typical of the alloy.
- The yield and tensile strengths of fiber laser deposited Inconel 718 and Waspaloy were well above the minimum values as defined in the aerospace specifications AMS 5596K and AMS 5544J, respectively. However, the elongations at fracture for both Inconel 718 and Waspaloy were slightly lower than the specified values for their wrought products as defined in AMS 5596K and AMS 5544J, respectively.

ACKNOWLEDGMENTS

The authors are grateful to E. Poirier and X. Pelletier for preparing the laser deposited specimens and their technical support during metallography preparation. Thanks are also due to E. Lebard and B. Villenave for their support related to metallographic examination and hardness testing.

REFERENCES

[1] J.N. Dupont, J.C. Lippold and S.D. Kiser, Welding Metallurgy and Weldability of Nickel-Base Alloys, John Wiley & Sons Inc., Hoboken, New Jersey, 2009.

[2] G.K.L. Ng, G.J. Bi and H.Y. Zheng, An Investigation on Porosity in Laser Metal Deposition, The International Congress on Applications of Lasers & Electro-Optics (ICALEO) Laser Materials Processing Conference, Paper #105, Temecula, California, Oct. 2008, pp. 23-30.

[3] H. Qi, M. Azer and A. Ritter, Studies of Standard Heat Treatment Effects on Microstructure and Mechanical Properties of Laser Net Shape Manufactured Inconel 718, *Metallurgical and Materials Transactions A*, Vol. 40A, 2009, pp. 2410-2422.

[4] J. Andersson and G.P. Sjoberg, Repair Welding of Wrought Superalloys: Alloy 718, Allvac 718Plus and Waspaloy, *Science and Technology of Welding and Joining*, Vol. 17, 2012, pp. 49-59.

[5] B. Baufeld, Mechanical Properties of Inconel 718 Parts Manufactured by Shaped Metal Deposition (SMD), *Journal of Materials Engineering and Performance*, 2011, Vol. 21, No. 7, 2011, pp.1416-1421.

[6] N.I.S. Nussein, J. Segal, D.G. McCartney, I.R. Pashby, Microstructure Formation in Waspaloy Multilayer Builds Following Direct Metal Deposition with Laser and Wire, *Materials Science and Engineering A*, Vol. 497, 2008, pp. 260-269.

[7] J.C. Ion, *Laser Processing of Engineering Materials; Principles, Procedure and Industrial Application*, Elsevier Butterworth-Heinemann, 2005.

[8] L. Quintino, A. Costa, R. Miranda, D. Yapp, Welding with High Power Fiber Lasers – A Preliminary Study, *Materials & Design*, Vol. 28, No. 4, 2007, pp. 1231-1237.

[9] H.C. Chen, A. Pinkerton, L. Li, Fibre laser welding of dissimilar alloys of Ti-6Al-4V and Inconel 718 for aerospace applications, *The International Journal of Advanced Manufacturing Technology*, Vol. 52, 2011, pp. 977-987.

[10] Y.N. Zhang, X. Cao, P. Wanjara and M. Medraj, Tensile properties of laser additive manufactured Inconel 718 using filler wire, Special issue: The Materials Science of Additive Manufacturing, *Journal of Materials Research*, Vol. 29, 2014, 2006-2020.

[11] Y.N. Zhang, X. Cao and P. Wanjara: Fiber laser deposition of Inconel 718 using filler wire, *Internation Journal of Advanced Manufacturing Technology*, Vol. 69, 2013, 2569.

[12] Y.N. Zhang, X. Cao, P. Wanjara and M. Medraj, Oxide Films in Laser Additive Manufactured Inconel 718, *Acta Materialia*, Vol. 61, 2013, pp. 6562-6576.

[13] G.D.J. Ram, A.V. Reddy, K.P.Rao, G.M. Reddy, J.K.S. Sundar, Microstructure and Tensile Properties of Inconel 718 Pulsed Nd-YAG Laser Welds, *Journal of Materials Processing Technology*, Vol. 167, 2005, pp. 73-82.

[14] G.D.J. Ram, A.V. Reddy, K.P.Rao, G.M. Reddy, Microstructure and Mechanical Properties of Inconel 718 Electron Beam Welds, *Material Science and Technology*, Vol. 21, No. 10, 2005, pp. 1132-1138.

[15] P.N. Quested, M. McLean, Effect of variations in Temperature Gradient and Solidification rate on microstructure and creep behaviour of IN738 LC, Solidification Technology in the Foundry and Cast House, The Metals Society Coventry England, 1980, pp. 586.

[16] L.O. Osoba, A Study on Laser Weldability Improvement of Newly Develop Haynes 282 Superalloy, PhD thesis, Department of Mechanical and Manufacturing Engineering, University of Manitoba.

[17] S. Kou, Welding Metallurgy, John Wiley & Sons Inc, 2002.

[18] G.A. Knorovsky, M.J. Cieslak, T.J. Headley, A.D. Romig, and W.F. Hammetter, Inconel 718: A solidification diagram, *Metallurgical and Materials Transactions A*, Vol. 20A, 1989, pp. 2149-2158.

[19] Y.N. Zhang, X. Cao, P. Wanjara and M. Medraj, Fiber Laser Deposition of Inconel 718 Using Powders, Advanced Materials, Processes and Applications for Additive

Manufacturing Symposium, Materials Science and Technology, 37-49, 2013, Montreal, Canada.
[20] Lippold JC, Recent Developments in Weldability Testing for Advanced Materials, ASM international, Joining of Advanced and Specialty Materials VII, 2005.
[21] Alloy IN-738 Technical Data, The international Nickel company (INCO), http://www.nipera.org/~/Media/Files/TechnicalLiterature/IN_738Alloy_PreliminaryData_497_.pdf